Supporting Information

Novel BODIPY-based MOFs toward High-Efficiency Photocatalytic Oxidation of Sulfides or Arylboronic Acids

Qian Kang, [a, †] Shao-Dan Wang, [a, †] Jie Guo, [a] Kai-Li Mo, [a] Kang-Le Lv [b] and Li-Li Wen [a,*]

[a] Engineering Research Center of Photoenergy Utilization for Pollution Control and Carbon Reduction, Ministry of Education; College of Chemistry, Central China Normal University, Wuhan, 430079, P. R. China.

[b] Key Laboratory of Catalysis and Energy Materials Chemistry of Ministry of Education, South-Central University for Nationalities, Wuhan 430074, P. R. China.

† These authors equally contributed to this work.

*Corresponding Author. E-mail: wenlili@mail.ccnu.edu.cn (L. L. Wen)

Experiment Section

General Procedures. All chemicals and solvents were commercially available and used as received. IR spectrum was recorded on a Bruker Tensor 27 spectrometer as dry KBr discs in the 400-4000 cm^{-1} region. All powder X-ray diffraction (PXRD) data were collected on a Bruker D8 Advance diffractometer using Cu Kα radiation and 2θ ranging from 5 to 40° at room temperature. The UV-vis diffused reflectance spectra (DRS) were obtained on an Agilent Cary 100 UV-vis spectrophotometer with $BaSO_4$ as the reference for the baseline correction. Electron paramagnetic resonance (EPR) spectra were obtained on a Bruker EMXmicro EPR under visible-light irradiation. Scanning frequency: 9.83 GHz; central field: 3508.25 G; scanning power: 0.2 mW; scanning temperature: 25 °C. Room temperature photoluminescence (PL) and Time-resolved photoluminescence (TRPL) spectra of of the samples were collected on a FLS 1000 fluorescence spectrophotometer. Gas chromatography (GC) was recorded on GC-2010 Plus under the following conditions: oven temperature 280 °C, injector temperature 250 °C, column temperature program 10 °C/min, from 150 to 280 °C holding for 15 min. The light irradiation was obtained by a 16 W blue LED. The electrochemical measurements were completed on a CHI760E electrochemical station in a standard three-electrode system with a graphite electrode (i.d. = 3 mm) as the working electrode system, a Pt electrode as the counter electrode, and an Ag/AgCl electrode as the reference electrode. Aqueous solution of Na_2SO_4 (0.5 M) was used as electrolyte.

X-ray Crystallography. The crystallographic data for compounds **1** and **2** was measured using a Bruker D8 Venture area-detector diffractometer with Ga-Kα radiation at 100 K. The structure was solved by direct methods and refined anisotropically with SHELXTL using full-matrix least-squares procedures based upon F^2 values. For compound **1**, the carboxyl group (C33, O3, O4 and C33A, O3A, O4A) is disordered over two positions with site occupancy factors of 0.77653 and 0.22347. As simplified, part (C33, O3, O4) was used to describe the structure in the manuscript. In the structure, free solvent molecules were removed using the SQUEEZE routine of PLATON, the subsequent refinements were based on the new data generated. Crystallographic data

has been deposited with the Cambridge Crystallographic Data Centre (CCDC): 2129046 (**1**) and 2171025 (**2**). Select bond lengths and angles are provided in Table S2.

Photocatalytic Activities' Evaluation. In a typical reaction for the oxygenation of sulfides, 3.0 mg of photocatalyst, 0.25 mmol sulfide and 1 mL of mixed solvent ($CH_3OH/CHCl_3$, v/v = 1:1) were introduced into a 10 mL Pyrex vial with a magneto. The Pyrex vial was then stirred magnetically for 5 min with 500 r/min in dark at ambient conditions. Subsequently, the photocatalytic oxidation was irradiated under visible light using a 16 W blue light-emitting diodes (LED). After completion of the reaction, *n*-decane as an internal standard was added into the tube, and next, the mixture was centrifuged to separate photocatalyst. Photo-induced catalytic reactions were monitored utilizing gas chromatography (GC) after filtration via a porous membrane with a diameter of 0.22 μm. The chemical structures of products were confirmed by comparison with standard chemicals. Similarly, for the photocatalytic oxidative hydroxylation of arylboronic acid, similar procedure was employed except that 3.0 mg of photocatalyst, 0.1 mmol arylboronic acid, 50 μL DIPEA (*N,N*-diisopropylethylamine) and 2.0 mL of solvent (CH_3CN) was introduced. The chemical structures of products were confirmed as compared to standard chemicals.

EPR Experimental. For the detection of $O_2^{\bullet-}$, 0.1 mL of 5,5-dimethyl-1-pyrroline *N*-oxide (DMPO)/DMF solution (30 μL/1.0 mL) was mixed with 1.0 mL of compound **1**/DMF (3.0 mg/1.0 mL), which was irradiated by a 16 W blue LED for 10 min at room temperature under air atmosphere, then sucking the filtrate with a 0.9 mm capillary tube transferred to EPR (electron paramagnetic resonance) tube for measurement. The detection of $^1O_2$ was conducted, employing the similar process but utilizing 2,2,6,6-tetramethylpiperidine (TEMP) as the trapping agent.

Recyclability of Oxidation of Thioanisole over Compound 1. After the reaction indicated above, the reaction solution was centrifuged at 6000 rpm for 3 min after each cycle and washed with CH_3OH 3 times. Then the catalyst was reused for the subsequent

run with fresh thioanisole (0.25 mmol) under the optimized reaction conditions. Recyclability of oxidative hydroxylation of phenylboronic acid was similar to recyclability of oxidation of thioanisole.

Electrochemical Measurements. The catalyst (10 mg) was dispersed in 20 μL of 5 wt% Nafion and 1 mL of H_2O/CH_3OH (v/v, 1:1) to obtain a suspension, and 20 μL of the suspension was scattered on the prepared graphite electrode then dried at room temperature in air. The Mott-Schottky plots were collected in 0.5 M Na_2SO_4 solution. The Mott-Schottky plots of compounds **1** and **2** were measured at frequencies of 500, 1000, and 1500 Hz. While the photocurrent signal measurement was performed with fluoride-tin oxide (FTO) glassy electrode (area of 0.8 cm^2) as the working electrode system under visible light from a 300 W xenon lamp with full spectrum.

Scavenger Experiments. A series of photocatalyst-free radical scavengers were used to control the photoactivity experiments, i.e., KI and $AgNO_3$ were employed as the scavenger of photogenerated holes and electrons, isopropanol (IPA) as the scavenger of hydroxyl radicals (•OH), catalase as the scavenger of hydrogen peroxide (H_2O_2), 1,4-benzoquinone (BQ) as the scavenger of superoxide radical species ($O_2^{\bullet-}$), and 1,4-diazabicyclo[2.2.2]octane (DABCO) as the scavenger of singlet oxygen ($^1O_2$). Attempts were carried out similarly to the photocatalytic experiments where the radical scavengers (1 equiv or 5 μL of catalase) were added to the reaction system.

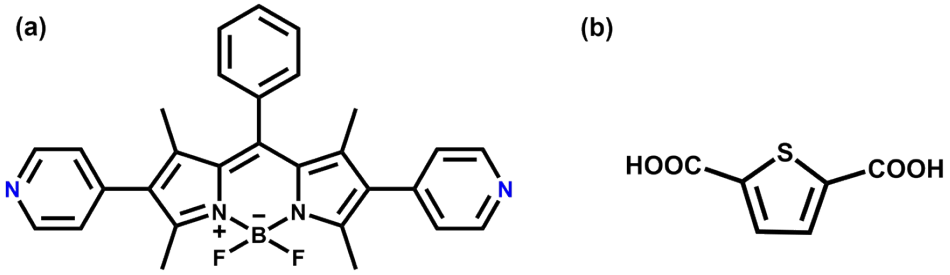

Scheme S1. The structure of (a) BODIPY and (b) H_2TDC.

Table S1. Crystallographic data and structure refinement for compounds **1** and **2.**

	Compound **1**	Compound **2**
Formula	$C_{35}H_{27}BF_2N_4O_4SZn$	$C_{35}H_{31}BCdF_2N_4O_6S$
Formula weight	713.84	796.91
Crystal system	monoclinic	monoclinic
Space group	*P*2/c	$P2_1/c$
a /Å	20.994(10)	16.1316(13)
b /Å	6.118(3)	11.5642(10)
c /Å	31.752(12)	19.1555(16)
α /°	90	90
γ /°	126.12(2)	99.8630(10)
β /°	90	90
V /Å^3	3294(3)	3520.6(5)
Z	4	4
ρ_{calcd}/g cm^{-3}	1.439	1.503
μ /mm^{-1}	3.145	0.740
Collected reflections	14100	35162
Unique reflections	5701	11508
R_1 [$I>2\sigma(I)$]	0.0452	0.0278
wR_2 (all data)	0.1022	0.0751
CCDC	2129046	2171025

Table S2. Selected bond distances (Å) and angles (deg) for compound **1**

Zn1−O2	1.985(2)	Zn1−N4	2.041(3)
Zn1−N1#1	2.067(3)	Zn1−O3	1.896(5)
O2−Zn1−N1#1	104.29(11)	O2−Zn1−N4	115.10(11)
N4−Zn1−N1#1	112.25(11)	O2−Zn1−O3	105.76(16)
O3−Zn1−N1#1	94.08(18)	N4−Zn1−O3	122.21(17)

#1 +*x*, -2-*y*, -1/2+*z*; #2 -*x*, +7, -3/2 -*z*; #3 +*x*, -2-*y*, 1/2+*z*

Table S3. Selected bond distances (Å) and angles (deg) for compound **2**

Cd1−O1	2.2480(13)	Cd1−O2#1	2.2948(13)
Cd1−O3#2	2.3379(13)	Cd1−O4#2	2.4806(14)
Cd1−N1	2.3032(13)	Cd1−N4#3	2.3391(13)
O1−Cd1−O2#1	102.15(5)	O1−Cd1−O3#2	90.61(5)
O1−Cd1−O4#2	143.48(5)	O1−Cd1−N1	107.34(5)
O1-Cd1-N4#3	85.78(5)	O2#1−Cd1−O3#2	163.21(5)
O2#1−Cd1−O4#2	110.57(5)	O2#1−Cd1−N1	90.30(5)
O2#1−Cd1−N4#3	82.79(5)	O3#2−Cd1−O4#2	54.41(5)
O3#2−Cd1−N4#3	87.38(5)	N1−Cd1−O3#2	96.32(5)
N1−Cd1−O4#2	88.65(5)	N1−Cd1−N4#3	166.26(5)

#1 2-*x*, 1-*y*, 1-*z*; #2 +*x*, 3/2-*y*, -1/2+*z*; #3 1+*x*, 1+*y*, +*z*; #4 +*x*, 3/2-*y*, 1/2+*z*; #5 -1+*x*, -1+*y*, +*z*;

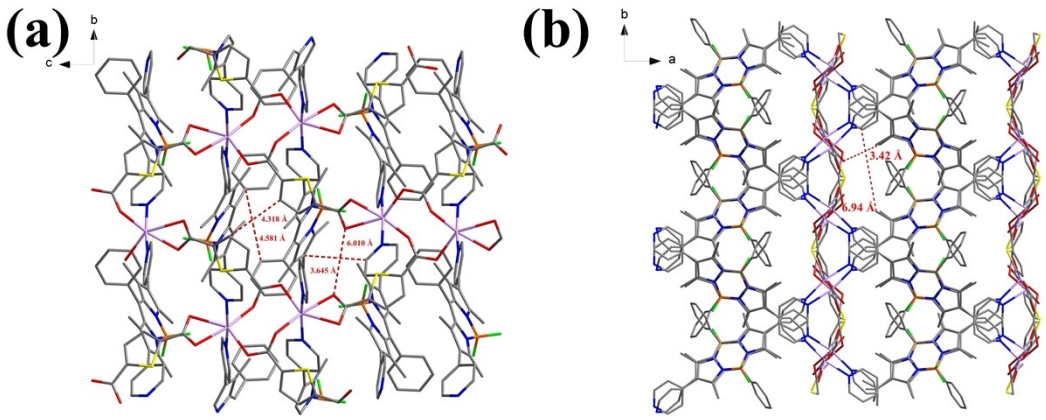

Figure S1 Presentation of the 3D architecture of compound **2** from (a) *a* axis and (c) *c* axis.

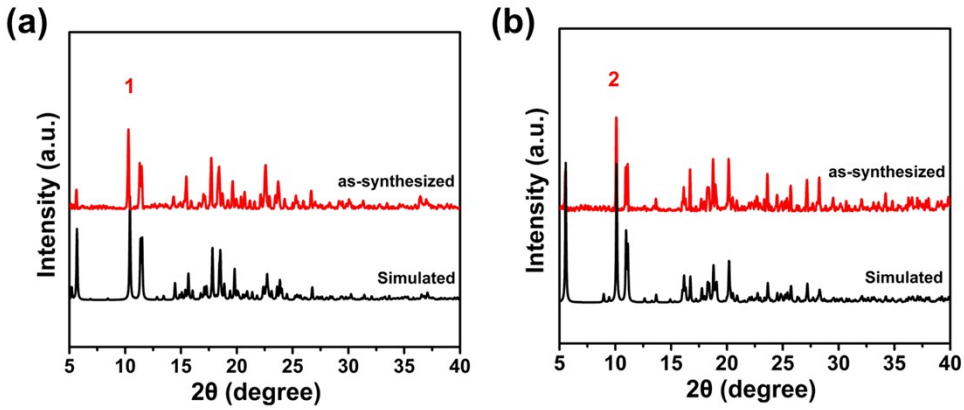

Figure S2. The PXRD patterns of (a) **1** and (b) **2** simulated spectrum was calculated from the single crystal data, respectively.

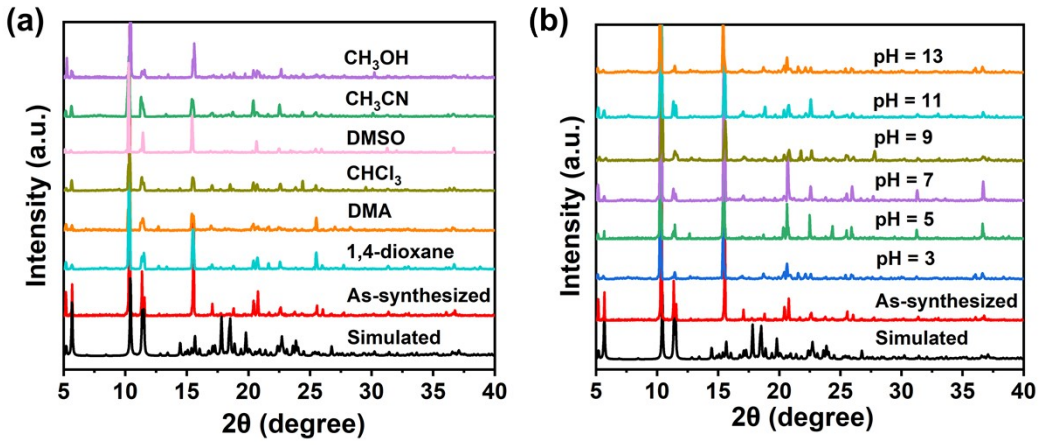

Figure S3. PXRD patterns of **1** in organic solvents (a) and in aqueous solution with pH range of 3-13 (b) for 48 h.

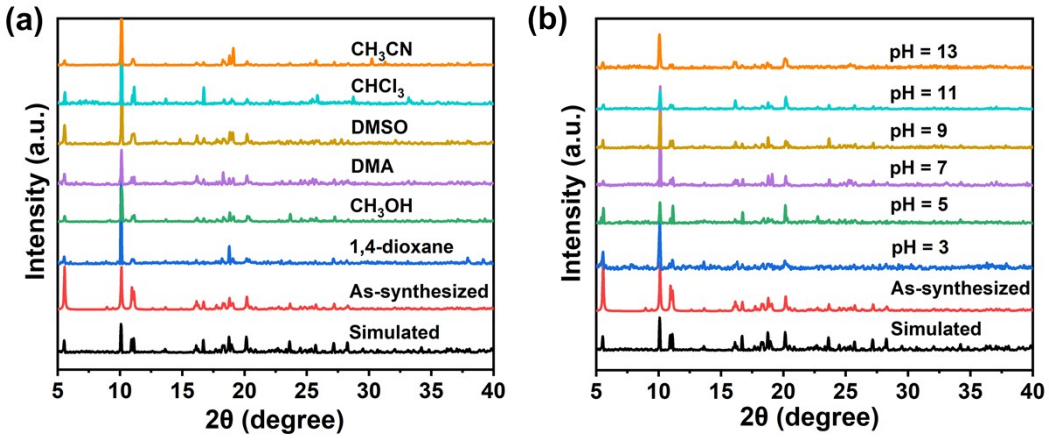

Figure S4. PXRD patterns of **2** in organic solvents (a) and in aqueous solution with pH range of 3-13 (b) for 48 h.

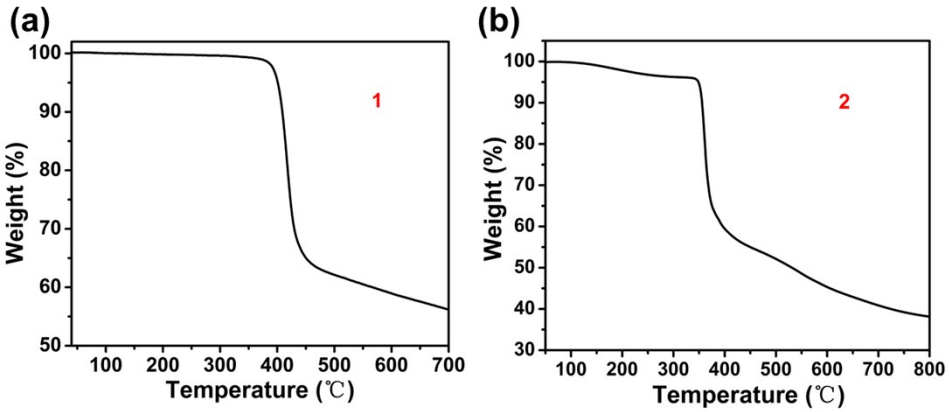

Figure S5. Thermogravimetric analysis (TGA) of (a) **1** and (b) **2.**

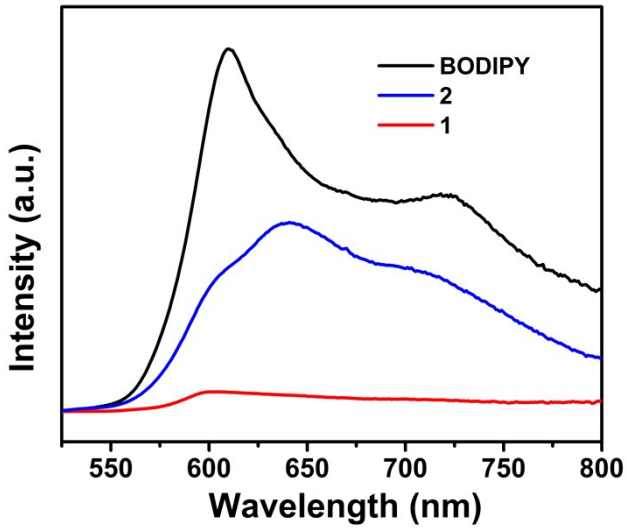

Figure S6. Steady-state photoluminescence spectra (PL) (excitation wavelength of 440 nm) of BODIPY, compounds **1** and **2.**

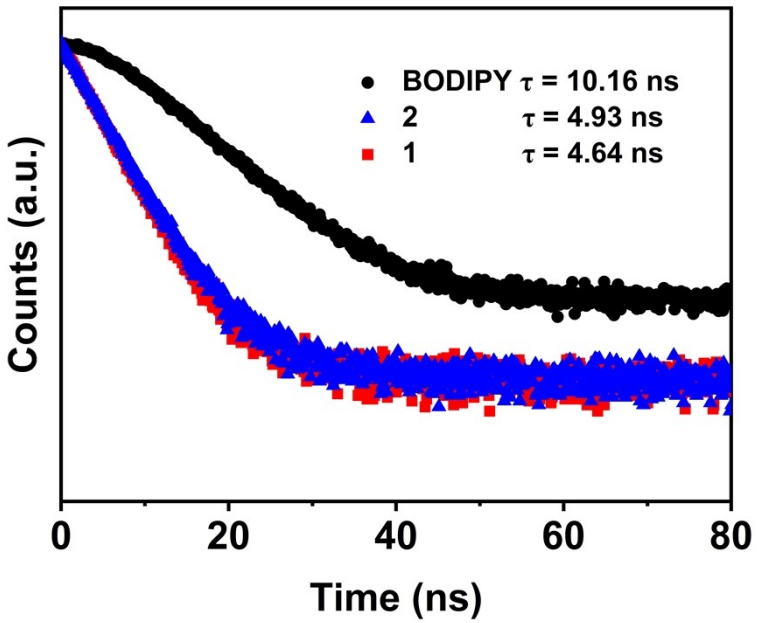

Figure S7. Time-resolved photoluminescence (TRPL) spectra of compounds **1**-**2** and BODIPY monomer.

Table S4 The calculated lifetimes of BODIPY and compound **1**-**2**.

	τ_1 (ns)	A_1	τ_2 (ns)	A_2	τ (ns)
BODIPY	6.62	-158198.39	6.83	162898.59	10.16
compound **1**					4.64
compound **2**					4.93

Note that, the TRPL spectra of compounds **1**-**2** followed a single exponential model, and BODIPY fitted a secondary exponential model. The lifetime of BODIPY was calculated according to the equation:

$$\tau = \frac{A_1\tau_1^2 + A_2\tau_2^2}{A_1\tau_1 + A_2\tau_2} \quad \text{(Equation R1)}$$

Table S5. Solvent influence on the photocatalytic oxidation of thioanisole over compound **1**.[a]

Entry	Solvent	Con. [%][b]	Sel. [%][b]
1	DMF	10	99
2	CH_3CN	96	93
3	CH_3CH_2OH	67	97
4	CH_3OH	85	88
5	$CHCl_3$	1	99
6	CH_3OH:$CHCl_3$	99	99

[a] Catalyst (3.0 mg), substrate (0.25 mmol), solvent (1.0 mL), 16 W blue LED, 1.5 h, air, 25 °C.

[b]Determined by GC using *n*-decane as the internal standard.

Table S6. Performances of the oxidation of thioanisole using various photocatalysts.

Catalyst	Light source	Oxidant	Time [h]	Conv. [%]	Sel. [%]	TOF [h^{-1}][a]	TOF [mmol g^{-1} h^{-1}][b]	Ref.
$[Zn_2(H_2O)_4Sn^{IV}(TPyP)(HCOO)_2]\cdot 4NO_3\cdot DMF\cdot 4H_2O$	350 W Xe lamp	O_2	12	>99.9	>99.9	0.8	—	1
UNLPF-10	Blue LED (135 mW, λ_{max} = 465 nm)	O_2	8	99	99	104.0	—	2
[Zn(ADBEB)(DMA)]	300 W Xe lamp	O_2	3.5	>99	>99	5.0	8.0	3
NNU-45	300 W Xe lamp (λ > 420 nm)	Air, H_2O_2	4	99	95	16.7	23.5	4
Zr_6-Irphen	Blue light LED (100 W, λ = 460 nm)	O_2	6	100	100	4.2	—	5
Zr-DTPP	25 W blue LED (5.0 mW/cm^2, 420 nm < λ_{em} < 490 nm)	O_2	7	97	—	692.9	—	6
Zr_{12}-NBC	24 W blue LED light	Air	10	100	100	5.0	—	7
Ru^{II} complex-based UIO-67	26 W fluorescent lamp	Air	22	72	—	16.6	—	8
P25 TiO_2	300 W Xe lamp (λ > 400 nm)	O_2	10	84	92	0.8	1.1	9
ARS-TiO_2	300 W Xe lamp (λ > 450 nm)	O_2	10	81	91	12.2	11.5	10
3%-C_{60}@PCN-222	LED lamp (50 mW/cm^2, λ > 400 nm)	Air	3	> 99	100	80.0	3.3	11
3D-PdPor-COF	3 W blue LEDs	Air	0.4	98	—	49.0	—	12
h-LZU1	300 W Xe lamp (λ > 380 nm)	Air (30 ℃)	22	100	92.6	—	1.3	13
DhaTph-Zn	300 W Xe lamp (λ > 400 nm)	1atm O_2	10	82	>99	—	0.41	14
C_3N_4 NSs-5 h	Xe lamp (λ > 400 nm)	0.1 MPa O_2	1	99	99	—	50.0	15
TTO-COF	blue LEDs (3 W × 4)	0.1 MPa O_2	2	90	98	—	26.5	16
Compound 1	**16 W blue LED lamps**	**Air**	**1.5**	**99**	**99**	**39.7**	**55.6**	**This work**

[a]TOF = mmol product/(mmol catalyst×reaction time).

[b]TOF = mmol product/(g catalyst×reaction time).

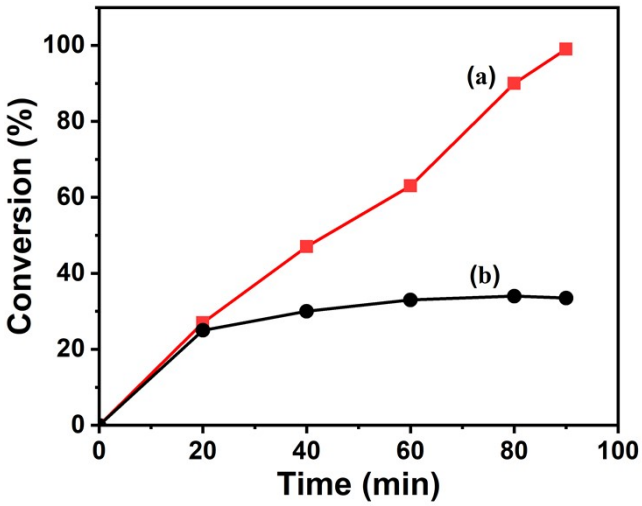

Figure S8. Leaching test for the oxidative of thioanisole over **1** under optimized reaction conditions. After 20 min of the reaction, the catalyst was filtered out whereas the filtrate was further reacted under identical conditions: (a) the common catalytic process and (b) hot filtration test.

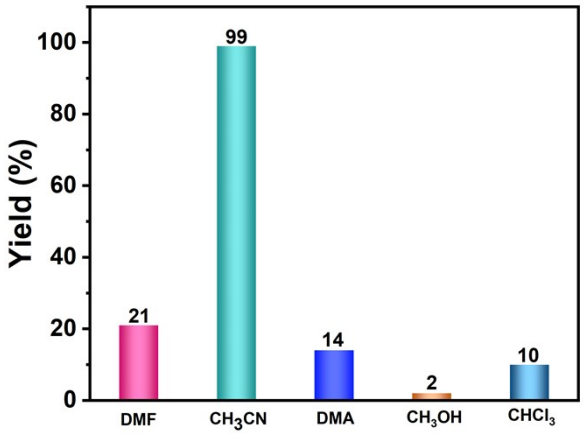

Figure S9. Solvent influence on the oxidative hydroxylation of phenylboronic acid over **1**.

Table S7. Performances of the photocatalytic hydroxylation of boronic acid using various photocatalysts.

Catalyst	Light source	Oxidant	Time [h]	Yield.[%]	TOF [h^{-1}][a]	TOF [mmol g^{-1} h^{-1}][b]	Ref.
JNU-204	30 W Blue LED	Air	48.0	93	1.9	10.4	17
MOF-525	Green LED	O_2	9.0	100	-	6.7	18
UiO-67-$Ru(bpy)_3$	23 W compact fluorescent bulb	Air	24.0	81	0.7	-	19
DhaTph-Ni	300 W Xe Lamp ($\lambda > 400$ nm)	O_2	1.5	99	-	6.6	14
COF-1	LED (440 nm)	Air	30.0	91	0.6	-	20
LZU-190	20 W white LED	Air	24.0	99	0.7	-	21
Cz-POF-1	14 W CFL	Air	24.0	94	2.0	-	22
BBO-COF	16 W white LED	Air	48.0	99	0.1	0.2	23
$[Ru(bpy)_3Cl_2]$ $\cdot 6H_2O$	36 W fluorescence lamp	Air	48.0	99	1.6	-	24
Compound 1	16 W blue LED	Air	1.5	99	15.9	22.2	This Work

[a]TOF = mmol product/(mmol catalyst×reaction time).

[b]TOF = mmol product/(g catalyst×reaction time).

References

(1) M.-H. Xie, X.-L. Yang, C. Zou and C.-D. Wu, A Sn^{IV}-Porphyrin-Based Metal-Organic Framework for the Selective Photo-Oxygenation of Phenol and Sulfides, *Inorg. Chem.*, 2011, **50**, 5318-5320.

(2) J. A. Johnson, X. Zhang, T. C. Reeson, Y.-S. Chen and J. Zhang, Facile Control of the Charge Density and Photocatalytic Activity of an Anionic Indium Porphyrin Framework via in Situ Metalation, *J. Am. Chem. Soc.*, 2014, **136**, 15881-15884.

(3) X. Liang, Z. Guo, H. Wei, X. Liu, H. Lv and H. Xing, Selective Photooxidation of Sulfides Mediated by Singlet Oxygen Using Visible-Light-Responsive Coordination Polymers, *Chem. Commun.*, 2018, **54**, 13002-13005.

(4) H. Wei, Z. Guo, X. Liang, P. Chen, H. Liu and H. Xing, Selective Photooxidation of Amines and Sulfides Triggered by a Superoxide Radical Using a Novel Visible-Light-Responsive Metal-Organic Framework, *ACS Appl. Mater. Interfaces*, 2019, **11**, 3016-3023.

(5) Li.-Q. Wei and B.-H. Ye, Cyclometalated Ir-Zr Metal-Organic Frameworks as Recyclable Visible-Light Photocatalysts for Sulfide Oxidation into Sulfoxide in Water, *ACS Appl. Mater. Interfaces*, 2019, **11**, 41448-41457.

(6) X. Feng, X. Wang, H. Wang, H. Wu, Z. Liu, W. Zhou, Q. Lin and J. Jiang, Elucidating J-Aggregation Effect in Boosting Singlet-Oxygen Evolution Using Zirconium-Porphyrin Frameworks: A Comprehensive Structural, Catalytic, and Spectroscopic Study, *ACS Appl. Mater. Interfaces*, 2019, **11**, 45118-45125.

(7) X.-N. Zou, D. Zhang, T.-X. Luan, Q. Li, L. Li, P.-Z. Li and Y. Zhao, Incorporating Photochromic Triphenylamine into a Zirconium-Organic Framework for Highly Effective Photocatalytic Aerobic Oxidation of Sulfides, *ACS Appl. Mater. Interfaces*, 2021, **13**, 20137-20144.

(8) C. Wang, Z. Xie, K. E. DeKrafft and W. Lin, Doping Metal-Organic Frameworks for Water Oxidation, Carbon Dioxide Reduction, and Organic Photocatalysis, *J. Am. Chem. Soc.*, 2011, **133**, 13445-13454.

(9) X. Lang, W. Hao, W. R. Leow, S. Li, J. Zhao and X. Chen, Tertiary Amine Mediated Aerobic Oxidation of Sulfides into Sulfoxides by Visible-Light Photoredox Catalysis on TiO_2, *Chem. Sci.*, 2015, **6**, 5000-5005.

(10) X. Lang, J. Zhao and X. Chen, Visible-Light-Induced Photoredox Catalysis of Dye-Sensitized Titanium Dioxide: Selective Aerobic Oxidation of Organic Sulfides, *Angew. Chem. Int. Ed.*, 2016, **128**, 4775-4778.

(11) D.-Y. Zheng, E.-X. Chen, C.-R. Ye and X.-C. Huang, High Efficiency Photo-Oxidation of Thioethers over C_{60}@PCN-222 Under Air, *J. Mater. Chem. A*, 2019, **7**, 22084-22091.

(12) Y. Meng, Y. Luo, J.-L. Shi, H. Ding, X. Lang, W. Chen, A. Zheng, J. Sun and C. Wang, 2D and 3D Porphyrinic Covalent Organic Frameworks: The Influence of Dimensionality on Functionality, *Angew. Chem. Int. Ed.*, 2020, **132**, 3653-3658.

(13) L. Liu, B. Zhang, X. Tan, D. Tan, X. Cheng, B. Han and J. Zhang, Improved Photocatalytic Performance of Covalent Organic Frameworks by Nanostructure Construction, *Chem. Commun.*, 2020, **56**, 4567-4570.

(14) Y. Qian, D. Li, Y. Han and H.-L. Jiang, Photocatalytic Molecular Oxygen Activation by Regulating Excitonic Effects in Covalent Organic Frameworks, *J. Am. Chem. Soc.*, 2020, **142**, 20763-20771.

(15) J. Li, Y. Chen, X. Yang, S. Gao and R. Cao, Visible-Light-Mediated High-Efficiency Catalytic Oxidation of Sulfides Using Wrinkled C_3N_4 Nanosheets, *J. Catal.*, 2020, **381**, 579-589.

(16) F. Zhang, H. Hao, X. Dong, X. Li and X. Lang, Olefin-Linked Covalent Organic Framework Nanotubes Based 0n Triazine for Selective Oxidation of Sulfides with O_2 Powered by Blue Light, *Appl.Catal. B: Environ.*, 2022*,* **305**, 121027.

(17) J. K. Jin, K. Wu, X. Y. Liu, Q. H. Guo, Y. L. Huang, D. Luo, M. Xie, Y. F. Zhao, W. G. Lu, X. P. Zhou, J. He and D. Li, Building a Pyrazole-benzothiadiazole-pyrazole photosensitizer into Metal-Organic Frameworks for Photocatalytic Aerobic Oxidation, *J. Am. Chem. Soc*., 2021, **143**, 21340-21349.

(18) T. Toyao, N. Ueno, K. Miyahara, Y. Matsui, T. H. Kim, Y. Horiuchi, H. Ikeda and M. Matsuoka, Visible-light, Photoredox Catalyzed, Oxidative Hydroxylation of Arylboronic Acids using a Metal-Organic Framework Containing Tetrakis (carboxyphenyl) Porphyrin Groups, *Chem. Commun*., 2015, **51**, 16103-16106.

(19) X. Yu and S. M. Cohen, Photocatalytic Metal-Organic Frameworks for the Aerobic Oxidation of Arylboronic Acids, *Chem. Commun*., 2015, **51**, 9880-9883.

(20) X. Kang, X. Han, Y. Chen, C. Cheng, Y. Liu and Y. Cui, Reticular Synthesis of Tbo Topology Covalent Organic Frameworks, *J. Am. Chem. Soc*., 2020, **142**, 16346-16356.

(21) P. F. Wei, M. Z. Qi, Z. P. Wang, S. Y. Ding, W. Yu, Q. Liu, L. K. Wang, H. Z. Wang, W. K. An and W. Wang, Benzoxazole-linked Ultrastable Covalent Organic

Frameworks for Photocatalysis, *J. Am. Chem. Soc.*, 2018, **140**, 4623-4631.

(22) J. Luo, X. Zhang and J. Zhang, Carbazolic Porous Organic Framework as an Efficient, Metal-free visible-light Photocatalyst for Organic Synthesis, *ACS Catal*., 2015, **5**, 2250-2254.

(23) X. Yan, H. Liu, Y. Li, W. B. Chen, T. Zhang, Z. Q. Zhao, G. L. Xing and L. Chen, Ultrastable Covalent Organic Frameworks via Self-polycondensation of an A_2B_2 Monomer for Heterogeneous Photocatalysis, *Macromolecules*, 2019, **52**, 7977-7983.

(24) Y. Q. Zou, J. R. Chen, X. P. Liu, L. Q. Lu, R. L. Davis, K. A. Jørgensen and W. J. Xiao, Highly Efficient Aerobic Oxidative Hydroxylation of Arylboronic Acids: Photoredox Catalysis using Visible Light, *Angew. Chem. Int. Ed.*, 2012, **51**, 784-78.